

See discussions, stats, and author profiles for this publication at: <https://www.researchgate.net/publication/267543051>

Numerical Approaches of Cluster Statistics for Stochastic Manganese Deposits

Article in *Zeitschrift fur Naturforschung a* · September 2014

DOI: 10.5560/ZNA.2014-0054

CITATION

1

READS

77

1 author:



Mehmet Bayirli

Balikesir University

36 PUBLICATIONS 96 CITATIONS

SEE PROFILE

Some of the authors of this publication are also working on these related projects:



Numerical study with scaling theory for the magnesite surface: Lacunary analysis [View project](#)

Numerical Approaches of Cluster Statistics for Stochastic Manganese Deposits

Mehmet Bayirli

Physics Department, Science and Art Faculty, Balikesir University, Balikesir, Turkey

Reprint requests to M. B.; E-mail: mbayirli@balikesir.edu.tr

Z. Naturforsch. **69a**, 581 – 588 (2014) / DOI: 10.5560/ZNA.2014-0054

Received April 4, 2014 / revised June 27, 2014 / published online September 10, 2014

In terms of origin, the most important manganese deposits are sedimentary deposits which grow on the surface and/or fractures of the natural magnesite ore. They reveal various morphological characteristic according to their location in origin. Some of them may be fractal in appearance. Although several studies have been completed with regards to their growth mechanism, it may be safe to say that their cluster statistics and scaling properties have rarely been subject an academic scrutiny. Hence, the subject of this study has been designed to calculate cluster statistics of manganese deposits by first; transferring the images of manganese deposits into a computer and then scaling them with the help of software. Secondly, the root-mean square (rms) thickness (also called as expected value in systems), the number of particles, clusters and cluster sizes are computed by means of scaling method. In doing so it has been found that the rms thickness and the number of particles are in correlation, a result which is called as power-law behaviour, $T \sim N^{-\varepsilon}$ (the critical exponent is computed as $\varepsilon = 1.743$). It has also been found that the correlation between the number of clusters and their sizes are determined with the power-law behaviour $n(s) \sim s^{-\tau}$ (the critical exponent τ may vary between 1.054 and 1.321). Finally, the distribution functions of natural manganese clusters on the magnesite subtract have been determined. All that may point to the fact that the manganese deposits may be formed according to a Poisson distribution. The results found and the conclusion reached in this study may be used to compare various natural deposits in geophysics.

Key words: Structure of Minerals; Numerical Methods; Critical Exponents.

PACS numbers: 91.60.Ed; 02.60.-x; 64.60.F-; 61.43.Hv

1. Introduction

The pattern formation of natural or artificial deposits on surfaces is subject to a considerable interest in many diverse areas of the literature such as geophysical sciences [1, 2]. The results found may be applied in several areas. One such important natural pattern is known as manganese deposits (MnDs) [3]. These amazing patterns of MnDs, also called macros crystalline, may be fractal in appearance [4]. They may be found on the surface and/or fractures of the natural magnesite ore (MO) deposits [5], some agates [5, 6], lime stones [7], and vein quartz [8]. Depending on their location of origin, they may grow in the form of several morphological phases such as dendrites, needles, dense branching, string-like, and compacts [2–8].

The questions of how MnDs' have been formed and what kind of scaling properties they reveal are

still hotly discussed in the geophysical science [3–8]. So far several studies have been concluded in order to clarify the growth mechanisms of MnDs some of which employed simulations, numerical computations, and experiments. Of those simulations some has been done on two-dimensional (2D) surfaces such as diffusion limited aggregation (DLA) proposed by Witten and Sander [9] and diffusion-reaction aggregation (DRA) presented Chopard et al. [5]. Studies determining the fractal dimensions and the shape parameters of MnDs (patterns on the MO surface and vein quartz surface [4–8]) have been done by Bayirli [7] and Ng and Teh [8], respectively, using numerical methods. Meanwhile, experimental studies observing the tree-like MnDs patterns have been performed by García-Ruiz et al. [6] and Xu et al. [3]. A reservoir was filled with a colloidal suspension of MnOOH and FeOOH oxide particles by García-Ruiz et al. [6]. Then three glass disks were piled and the surfaces between them

coated with tooth paste (colloidal soda). The pile was immersed in the manganese solution and then a set of fractures was provoked by impacting a hammer on the glass pile. After a while tree-like patterns were observed on the silica thin layers [6]. Xu et al. characterised tree-like MnDs on three different substrate rocks (rhyolite, clayey siltstone, and limestone) via high-resolution electron microscopy and found that the tree-like MnDs are mainly composed of nanometres scale manganese-(hydr) oxides, iron-(oxy) hydroxide, sulphate, and clay minerals. Each of these samples revealed different main manganese phases. Chain-width disorder and chain termination occurred in some samples such as todorikite. Todorikite crystals showed trilling inter growths. The chain termination rule for the tree-like MnDs was explained by the geometry of octahedral chains and octahedral wall layer. It was also suggested that the formation mechanism of todorikite might have been transferred from birnessite [3].

In many cases, the MnDs grow under non-equilibrium conditions and reveal self-similarity patterns. Yet only a limited number of works may be found in the literature studying the characteristics of MnDs' emerging on natural MOs using numerical approaches such as scaling analysis and statistical computations. Even though MnDs patterns are considered and tented by geologists as rather meaningless structures due to the indefiniteness of their geneses, determining their genesis may still be of great practical importance especially in figuring out of the growth mechanism of the geological environments.

Scaling and self-affinity are important notions in geophysics [1, 2, 10]. They are generally described with simple power laws which consists of exponentiation (defined as scaling exponent). Determining a simple power law is usually done without consideration to the details of experiments and nature such as growth conditions and specific experimental systems [9].

For example, Meakin has reported a scaling exponent for the patterns obtained by a DLA model in 2D using Monte Carlo method [11]. Meanwhile, a tree-like pattern obtained by means of electro deposition method from the zinc metal is presented by Matsushita et al. [12]. As patterns of MnDs are of natural growth (in natural conditions) as well as their morphological structure may show evidence of the scaling and self-affine properties, unrelated to formation details, scaling treatments have been chosen as a method of analyses in this study [1, 2, 10].

With respect to that, the scaling properties and cluster statistics of MnDs patterns on the surface of MOs are estimated by means of various numerical origins. For that, the root-mean square (rms) thickness (also called as expected value in systems), the number of particles, clusters and cluster sizes are computed by means of the scaling method, thus determined the relationship between the number of particles and the cluster sizes. All that may reveal the contribution of the geological environments for the growth of MnDs. They may also be useful for comparing similar experimental results such as nickel, and the nickel-phosphate film (electro deposited under galvanic static conductions).

2. Scaling Method

Surfaces of MO deposits with different distribution properties of MnDs have been scanned with an Epson Stylus DX485 scanner and the images obtained have been fed into a personal computer. A typical image of a MO surface is shown in Figure 1. A difference between the brightness of MnDs and other regions may be observed due to the diversity of the surface of the MO deposits. The high contrast in the MO images can be clearly differentiated both within the magnesite and manganese deposits, varying from bright to dark. The MnDs are distributed randomly on the surface and/or fractures of the MO. Then these images are fed into the computer software for processing. In an attempt to differentiate the samples, they are flittered by the Gaussian blur method as $\sigma = 2$. Finally, MnDs images in the BMP format are converted into 8 bits so



Fig. 1. Typical magnesite ore surface with MnDs. The MnDs patterns are distributed as random structure on the MO surface.

that the MnDs and the number of the particles may be counted.

3. Results and Discussion

Numerical computations for determining the cluster statistics and scaling properties of MO surfaces of the MO have been carried out on a finite square lattice. Four different square areas have been selected from two dissimilar MO images according to the distribution of the MnDs patterns and their complexity. The linear dimension of finite-size square lattices has been taken as $L = 256$ pixel. MO image samples have been transformed into binary images, labelled as MnDs-A, MnDs-B, MnDs-C, and MnDs-D and finally scaled linearly by means of the software used. The MnDs patterns have been observed as a dark colour in each pixel on the surfaces of the MO. The bright colours have been characterized for the magnesite. In the final, MnDs structures have been observed in various morphological characteristics such as DLA-like, dendrite, needle, dense branching, compact, and string-like structures as seen on the surface of some electrodeposits. In previous studies the shape parameters (i.e. fractal dimensions and divergent ratios) had been computed and presented [4–8]. Therefore, in this study, the cluster statistics and scaling properties of MnDs (found on the surface with various geometrical structures, different cluster sizes, and cluster distribution) have been determined.

The MO surfaces can be determined as a value of two occupied fractions [1, 2]. First; the occupied fraction of MnDs' particles on the MO surface \bar{h} is given as

$$\bar{h}(L, h) = (L^{-d}) \sum_{j=1}^L \sum_{i=1}^L x_{i,j}, \quad (1)$$

where $N = \sum_{j=1}^L \sum_{i=1}^L x_{i,j}$ is the total cumulative site of the MO surface according to the BMP format in binary scale. The value of \bar{h} is computed as varying from 0.13 to 0.16.

Secondly, the cluster density \bar{n} is related to the number of the MnDs $n(s_i)$ and their geometrical structures [1, 2, 4]. The cluster density can be determined as

$$\bar{n} = n^{-d} \sum_{j=1}^n n(s_j), \quad (2)$$

where n and $n(s_i)$ stands for the total number of cumulative clusters and the number of clusters in cluster size s_i , respectively. The cluster density is defined by the ratio of cluster numbers to the number of total pixels on the surface. The number of total pixels on the sample images is computed from the finite size square of the MO. Their value varies from 27 200 to 352 965. While the cluster size increases the cluster density decreases. This is an expected result [1, 2]. However, as the particle density increases, the number of clusters is reduced on the MO surfaces.

The root-mean-square (rms) thickness is an important concept for the statistical computations. Therefore, the rms thickness $T(h)$ is computed according to the number N of particles on the MnDs. The rms thickness is also characterized as the square root of the mean value for the squares of the distance points from the image mean value. This is identified as the statistical expected value in the system [1, 2, 4, 10]. A distinct approximation of $T(h)$ on the pattern of the surfaces is defined by

$$T(L, h) = \left[(L^{-d}) \sum_{i=1}^N \sum_{j=1}^N (x_{i,j} - \bar{h})^2 \right]^{1/2}, \quad (3)$$

where L , d , and $x_{i,j}$ is the linear dimension, the Euclidian dimension, and the height value at each data points in the MO image, respectively. The height value for the particle density in each pixel on the image of the MO surface array $\rho(x_{i,j})$ is defined as

$$\rho(x_{i,j}) = \begin{cases} 1 & \text{if dark pixel exists } x_{i,j}, \\ 0 & \text{if bright pixel exists } x_{i,j}. \end{cases} \quad (4)$$

The rms thicknesses according to occupied fractions \bar{h} and the total number of particles N are computed and then both averaged over various MnDs' samples by selecting an approximately equivalent size for each sample. The results indicate that, when the total number of cumulative cluster is increased in the MO surface (in the limit $n \rightarrow \infty$), the value of $T(N)$ is affected to both to the occupied fraction and the number of MnDs particles N . This relationship is defined as power law,

$$T(N) \propto N^\varepsilon, \quad (5)$$

where ε is the critical exponent for the samples. The critical exponent is computed as $\varepsilon = 1.743 \pm 0.327$. Figure 2 shows the dependence of $\log T$ to $\log N$ such

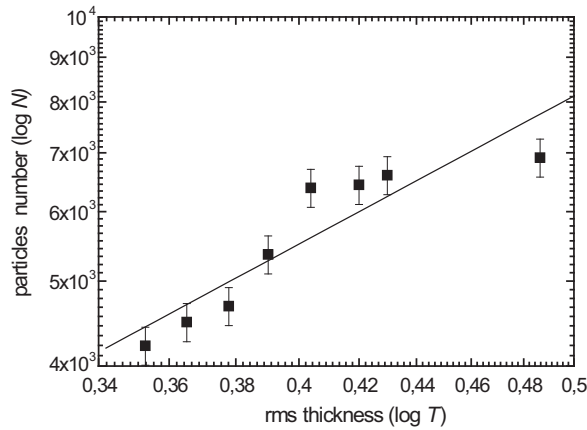


Fig. 2. A typical result of the relationship between rms thicknesses of the pattern of MnDs which are presented in Figure 1.

as in the DLA model. Having employed the Monte Carlo method, Meakin reported ε as 1.36 and 1.55 for the clusters obtained with the DLA model in 2D by using two different numerical approaches [11]. The critical exponent value ε of the MnDs is greater than those that are obtained via the DLA Model. DLA clusters are generally part of the surface which is subject to investigation. However, the MnDs on the surface of the MO are distributed randomly. The MnDs may vary in size according to the surface location. Meanwhile the critical exponent is reported by Matsushita et al. as $\varepsilon = 0.72$ for the three-like patterns of the zinc metal produced by the electro deposition method [12]. The value of ε was reported by Saitou and Okudaira as 0.9 for the Ni-P films deposited under galvanostatic conditions [10]. As for the MnDs (shown in Fig. 2), the

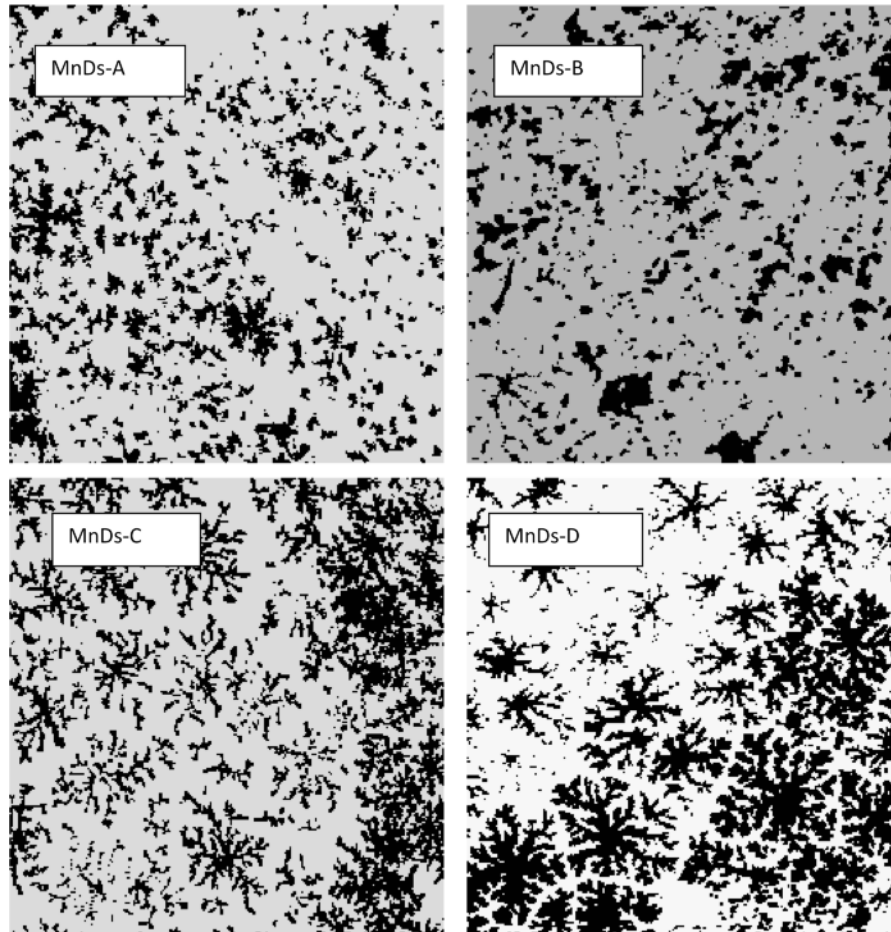


Fig. 3. Dark-bright images of a typical MO surface in BMP format. Their linear dimension are taken as $L = 256$ pixels.

value of ε is about 1.743, a number which is comparatively much bigger than the DLA and the tree-like zinc deposits. This finding indicates that the density of the MnDs' deposits increases during the deposition process.

Furthermore, the critical exponent ε is related to the effective fractal dimension (EFD) D_c for the MnDs. The relationships in geometric scaling between the rms thickness T and the numbers of particles N (first proposed by Meakin to estimate the EFD) are defined as characteristic of fractals and may be used to estimate an EFD D_s for the DLA deposits. The theoretical value of D_s is about $5/3 \cong 1.666$ [11] in 2D. This scaling relationship between T and N is also defined as power law. It is described as

$$T \sim N(s_i)^{1/(1-d+D_s)}, \tag{6}$$

where D_s stands for the EFD and d for the space dimension. MnDs are deposited on the consuetudinary flat surface of the natural magnesite ore ($d = 2$). This argument is also supported with the results obtained in this study (see Fig. 3). If (6) is used to estimate the EFD (if $D_c = D_s$ and $D_s = d - 1 + \varepsilon^{-1}$) for the MnDs on the magnesite ore, the EFD is computed as about 1.5737235. The EFD value is smaller than DLA in the present study. Because clusters of DLA may be represented as part of the manganese deposits on the MO surface. The obtained results more or less agree with both this theoretical values and the results obtained from a large-scale computer simulation performed by Meakin [11].

The other property of cluster formation is that: when manganese and iron ions in mineral solutions arrive at the magnesite and between the surface layers, they attach themselves to the surface or layers as a result of natural conditions and local effects such as the surface tension and surface defects. Since the ions on the surface are deposited and percolated, the critical exponent of MnDs is bigger than the DLA deposits [11].

The average value of cluster size is computed in the current scale. The size of the clusters growing on the MO surface may vary in value as they are produced from a stochastic process. The cluster size of the MnDs is related to width, thickness of the gap, and the roughness of the MO surfaces. The pressure formed by the sediment fluid and the viscosity of the pushed fluid may determine the parameters controlling both the scale and shape of the cluster sizes (such as

dendritic, non dendritic, compact, and needle-like patterns) [10, 12]. The correlation between the shape of MnDs and the natural conditions may also be observed in various systemic experiments [6, 12, 13]. It has been recognized that a wide variety of cluster patterns is controlled by the strength of a gradient which is found on a surface and interface field. The size of the cluster growth is dependent on the gradient of implied voltage in electro-chemical deposition, the pressure gradient in viscous fingering, and the temperature gradient in solidification [12, 13]. The cluster of MnDs is proportional to the concentration of the diffusing particles in the aggregation process of MnDs [6]. The average cluster size may generally be defined as

$$\bar{s} = n^{-1} \sum_{i=1}^n n(s_i)(x_{i,j}), \tag{7}$$

where n is the number of the clusters on the MO. Their values are computed as varying from 27 299 to 352 965 pixels. s is associated with the manganese formation in the surface location and the surface fractures.

For each sample, the size of the patterns of the MnDs on the MO surface and the number of the patterns $n(s_i)$ have been computed independently in order to clarify the relationship between them. The data obtained for the samples is found to be in great fluctuation.

The relationship between the number of MnD patterns and the pattern size of $s \geq 1$ pixels on finite size square lattice exhibits the scaling behaviour and may be defined as

$$n(s_i) \sim s^{-\tau}, \tag{8}$$

where τ is the critical exponent according to the scaling theory [1, 2, 12]. This relationship exhibits the scaling behaviour about $s \leq 30$ in the initial region of the available value for the cluster size s . The values of the critical exponent for each sample are computed as 1.054, 1.099, 1.252, and 1.321 for the MnDs-A, MnDs-B, MnDs-C, and MnDs-D, respectively. Employing the Monte Carlo method, Meakin reported the critical exponent τ as 1.55 for the clusters obtained with the DLA model in 2D [11]. Meanwhile, Matsushita et al. reported the critical exponent value of τ as 1.54 for the three-like patterns of the zinc metal obtained by electro deposition method [12]. In this study, the scaling behaviour disappears as a result of the irregular cluster size growth and the finite-size effect. The deviation of

Table 1. Values for the occupied fraction, the pattern number, the average size, the critical exponents, and the linear regression coefficients for the MnDs on the MO surface.

| Samples | \bar{h} % | Cluster numbers $n(s)$ | Average size (\bar{s}) | Critical exponents (τ) | Regression coefficients (r^2) |
|---------|-------------|------------------------|----------------------------|-------------------------------|-----------------------------------|
| MnDs-A | 13.080 | 314 | 27.299 | 1.054 ± 0.084 | 0.92136 |
| MnDs-B | 12.769 | 269 | 31.108 | 1.099 ± 0.091 | 0.86947 |
| MnDs-C | 16.467 | 115 | 93.783 | 1.252 ± 0.129 | 0.87359 |
| MnDs-D | 16.542 | 27 | 352.965 | 1.321 ± 0.111 | 0.90881 |

the scaling behaviour for the small values in the pattern size comes from the difficulty in counting small patterns. The results are shown in Figure 4 and summarised in Table 1.

Also, Rácz and Vicsek proposed that the value of the critical exponent τ is related to the EFD D_c and the Euclidian dimension d -space [14]. This relationship is defined as

$$\tau = 1 + \frac{d-1}{D_c}. \quad (9)$$

Assuming that $d = D_c$ and $D_s \cong 1.71$ (obtained from the simulation via the DLA model in two dimensions and from recent theoretical studies) [9], the predicted value of τ is about 1.5847953. Alternatively, the EFD D_c may be computed by using the value of τ as well as from the following equation $D_c = (d-1)/(\tau-1)$ from (9). Even though this technique is useful to calculate the fractal dimension of the DLA clusters, it may not be so to obtain accurate results in calculating the fractal dimension of MnDs. Because the cluster-size distribution and results of previous studies are indicated in

DLA contain only a small patch of the whole information concerning the aggregate structures.

The relationship between the number of pattern $n(s_i)$ and the cluster size s_i is related to the cluster-size distribution (CSD). The CSDs for the particle groups and the islands are proposed by Rácz and Vicsek as two exponents scaling form according to the computer simulations of two-dimensional DLA for an analogy with the equilibrium percolation problem [15]. They are defined as

$$n(s) \sim s^{-\tau} f(s^\sigma N^{-1}), \quad (10)$$

where τ , σ are the scaling exponents. $f(x = s^\sigma N^{-1})$ is defined as cutoff function. The value of the cutoff function is about $f(x) \approx 1$ for $x \ll 1$ and $f(x) \ll 1$ for $x \gg 1$ [15]. The cutoff function may also be argued to determine the numerical relationship between the number of clusters $n(s)$ and cluster-size value s_i as a mathematical model. $n(s_i)$ may be accepted as an approach for estimating the initial parameter function as the second order of the exponential distribution by us-

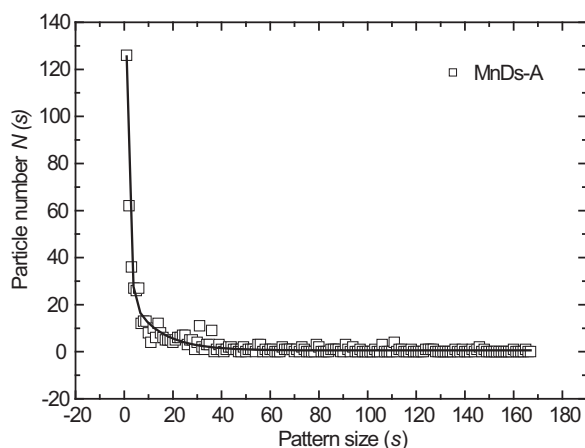


Fig. 4. Size of clusters observed on the MO surface as a function of the number of clusters. The fitting result is to the second order of the exponential decay using the nonlinear regression method.

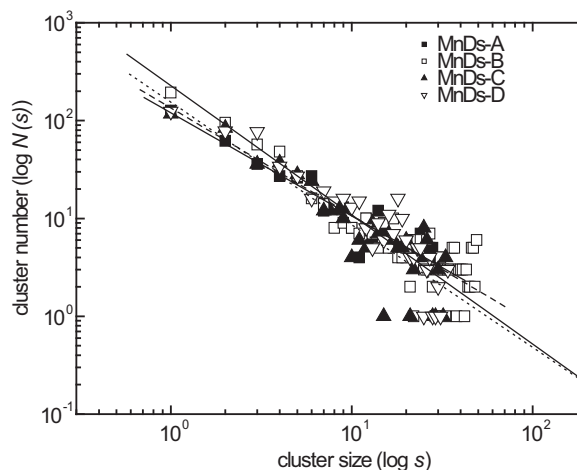


Fig. 5. A typical result of the cumulative number $n(s)$, the total number of the MnD patterns consisting of more than $s_i \geq 1$ pixels. It is a function of the size of s but the scaling behaviour has disappeared as about $s \geq 30$ pixels.

Table 2. Mathematical model parameters for the pattern-size distribution for the MnDs on the MO surface.

| Samples | n_0 | A_1 | t_1 | A_2 | t_2 | r^2 |
|---------|--------------------|---------------------|--------------------|---------------------|--------------------|---------|
| MnDs-A | 0.029 ± 0.007 | 243.691 ± 2.534 | 1.162 ± 0.013 | 23.532 ± 0.461 | 14.736 ± 0.288 | 0.97213 |
| MnDs-B | 0.0287 ± 0.008 | 341.898 ± 1.678 | 1.516 ± 0.009 | 13.460 ± 0.343 | 22.546 ± 0.610 | 0.98999 |
| MnDs-C | 0.0246 ± 0.008 | 8.401 ± 0.309 | 30.695 ± 1.203 | 174.552 ± 1.121 | 2.144 ± 0.019 | 0.97432 |
| MnDs-D | 0.014 ± 0.001 | 20.009 ± 0.765 | 15.206 ± 0.475 | 168.661 ± 1.124 | 2.145 ± 0.027 | 0.97407 |

ing nonlinear regression method in the following form

$$n(s) = n_0 + a_1 e^{-\frac{s}{t_1}} + a_2 e^{-\frac{s}{t_2}}, \tag{11}$$

where n_0 , a_1 , t_1 , a_2 , and t_2 are the nonlinear regression parameters, respectively. The model parameters are computed for the samples and the obtained results are presented in Table 2. The values of the regression coefficients r^2 are computed. The results showed that their values varied from 0.97407 to 0.98999.

The cluster mass m on the surface may be determined as

$$m \propto n(s_i)x_{i,j}. \tag{12}$$

This equation implies that the distribution of each accumulated pixel is determined only by multiplying $n(s_i)$ according to the stochastic process [15]. The mean values \bar{s} and standard deviation σ are defined as

$$\bar{s} = \sum_{i=1}^n h_i P_i \tag{13}$$

and

$$\sigma^2 = \sum_{i=1}^n (x_{j,i} - \bar{h})^2 P_{i,j}, \tag{14}$$

where $P_{i,j}$ is a probability density function. Nevertheless, the values of mean and standard deviation of the accumulated pixels in the MnDs may be written in the format

$$\bar{s} \propto \bar{h} \text{ and } \sigma^2 \propto (\bar{h})^2 \tag{15}$$

as expected results. These expected values are associ-

ated with h . They are obtained only when $P_{i,j}$ is a form of the following power distribution:

$$P_{i,j} = h^{-1} \exp(h^{-1}x_{i,j}). \tag{16}$$

The power distribution implies that the MnD pattern are independent of each other and may be distributed according to the Poisson distribution.

4. Conclusion

The primary objective of this study was to determine the cluster statistics and scaling properties of MnDs found on the surface of MO by means of numerical computations. With that objective the rms thickness, the number of particles, the occupied fraction of the particles, the cluster density, and the cluster size of MnDs have been computed via scaling method. The relationship between the rms thickness and the particle numbers show a scaling behaviour. The critical exponent in that scaling behaviour for the MnDs found on the surface of MO is computed as about 1.743. The relationship between the number of clusters and the cluster sizes also reveal a scaling behaviour. It is computed that, according to size of clusters and the particle density, the critical exponent may vary from 1.054 to 1.321. The cluster-size distribution may be determined according to the second order of the exponential distribution using nonlinear regression method. The MnDs' growth may occur according to the Poisson distribution. This argument is supported with stochastic theory and percolation process. The MnDs formation and solidification process may be investigated in great detail by a future study.

[1] A. L. Barbarasi and H. E. Stanley, Fractal Concepts in Surface Growth, Cambridge University Press, Cambridge 1995.
 [2] T. Vicsek, Fractal Growth Phenomena, Word Scientific, Singapore 1992.

[3] H. Xu, T. Chen, and H. Kanishi, American Mineralogist **95**, 556 (2010).
 [4] M. Bayirli and T. Ozbey, Z. Naturforsch **68a**, 405 (2013).

- [5] B. Chopard, H. J. Herrmann, and T. Vicsek, *Nature* **353**, 409 (1991).
- [6] J. M. García-Ruiz, F. Otálora, A. Sanchez-Navas, and F. J. Higes-Rolando, in *Fractals and Dynamics Systems in Geosciences*, ed. by J. H. Kruhl, Springer, Berlin 1994, pp. 307–318.
- [7] M. Bayirli, *Physica A: Statistical Mechanism and its Applications* **353**, 1 (2005).
- [8] T. F. Ng and G. H. Teh, *Geological Society of Malaysia* **55**, 73 (2009).
- [9] T. A. Witten and L. M. Sander, *Phys. Rev. Lett.* **27**, 5786 (1983).
- [10] M. Saitou and Y. Okudaira, *J. Elec. Chem. Soc.* **151**, C674 (2004).
- [11] P. Meakin, *Phys. Rev. B* **30**, 4207 (1984).
- [12] M. Matsushita, Y. Hayakawa, and Y. Sawada, *Phys. Rev. A* **32**, 63814 (1985).
- [13] B. Stegemann, C. Ritter, B. Kaiser, and K. Rademan, *J. Phys. Chem. B* **108**, 14292 (2004).
- [14] Z. Rácz and T. Vicsek, *Phys. Rev. Lett.* **51**, 2382 (1983).
- [15] H. M. S. Taylor and S. Karlin, *An Introduction to Stochastic Modeling*, 3rd edn., Academic Press, California, USA 1998.